

# ANALYSIS, DESIGN AND OPTIMIZATION OF A NONLINEAR ENERGY HARVESTER

Diala Uchenna, Pope Simon and Lang Zi-Qiang

*Department of Automatic Control and Systems Engineering, University of Sheffield, Western Bank, Sheffield, S10 2TN, UK*

*email: uhdiala1@sheffield.ac.uk*

This paper introduces the application of nonlinear damping in increasing the energy (power) harvested by a vibration-based energy harvester (VEH). It has been reported that when nonlinear cubic damping is employed in a VEH, more energy is harvested, at the resonant frequency, compared to linear damping, when the base excitation level exerted on the support-base of the VEH is below the maximum base excitation level the VEH is subjected to. The maximum base excitation level commensurately causes a maximum displacement of the harvester mass as the VEH is limited in its size and enclosure by design. This study focuses on the analysis and design of a VEH using a nonlinear frequency analysis method. The concept of the output frequency response function (OFRF) is employed to derive an explicit polynomial relationship between the harvested energy and the parameter of interest of the VEH which is the nonlinear damping coefficient. However this is subject to a maximum allowable displacement of the mass of the harvester. Due to this constraint, an optimization problem is posed. Based on the OFRF, an optimal nonlinear damping coefficient can be designed to realize a range of preferred energy levels subject to the mass displacement constraint of the VEH.

**Keywords:** Vibration, Vibration control, Vibration-based energy harvester, OFRF, Frequency domain methods, nonlinear vibration damping.

---

## 1. Introduction

The theory of Energy (power) harvesting from ambient vibration involves the conversion of kinetic energy, also known as ambient energy, to electrical energy. The vibration-based energy harvesting technology has been a hot topic in recent publications with some revealing results obtained. Sources of vibration like wind turbulence, ocean waves, automobile motion etc. provide mechanical energy which can be harvested and used for powering wireless sensors, wearable electronics etc [1, 2]. Most of the publications in literature have literally identified two major design limitations of energy harvesting systems. The first limitation is that energy harvesters are designed to function at a selected band of frequencies hence any source of vibration with disturbances having frequencies outside this band is untapped hence affecting the efficiency of the harvester system. However various nonlinear design concepts have been reported in literature to increase the excitation frequency range over which the harvester system is operational [3, 4]. The second limitation is the design constraint of the mass displacement as the harvester mass displacement is constrained due to the device size and geometry [3, 4]. Most harvester systems are employed in environments or structures subjected to fairly low vibration amplitudes hence they are designed for resonant levels to achieve maximum performance. Likewise, due to its proof mass displacement constraints, the harvester system is designed for the maximum excitation level the proposed operational region is subjected to.

It has been recently revealed in [5] that an introduction of a nonlinear cubic damping can extend the dynamic range of an energy harvester. In [5], using the harmonic balance method (HBM), the nonlinear energy harvester system with cubic damping was compared at resonance with a harvester system having an equivalent linear damper (providing same relative displacement as the nonlinear

harvester) and both systems were subjected to the maximum excitation level of the operational environment and lower excitation levels. It was shown that at the maximum excitation level, both systems harvested same energy (power) however at lower excitation levels, the nonlinear harvester extracted more energy.

The current study focuses on the analysis, design and optimization of a nonlinear harvester with cubic damping using a nonlinear frequency analysis method. The concept of the output frequency response function (OFRF) is employed to derive an explicit polynomial relationship between the harvested energy (power) and the VEH parameter of interest i.e. the nonlinear damping coefficient, subject to the proof mass displacement constraint. This, as reveals, poses a constrained optimization problem.

## 2. Model formulation

The vibration-based energy harvester system considered in this study include a base-excited single-degree-of-freedom (SDOF) mass-spring-damper system. This is illustrated in the schematic form as shown in Fig. 1.

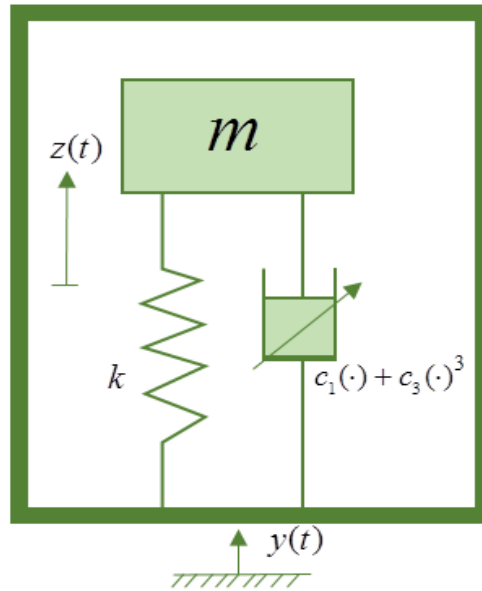


Figure 1: SDOF base excited VEH with nonlinear cubic damping.

As seen in Fig. 1, the SDOF energy harvester system comprises a proof mass  $m$  supported by vibration isolation elements which comprises a spring with stiffness  $k$ , linear and nonlinear dampers with damping coefficients,  $c_1$  and  $c_3$  respectively.

Given a base-excitation of  $y(t)$  exerted on the base of the harvester which results to a relative displacement of  $z(t)$  between the mass and the base of the harvester with the assumption that the base-excitation is harmonic in nature with magnitude and frequency  $Y$  and  $\omega$  respectively, then the system model of the SDOF VEH can be given as

$$m\ddot{z}(t) + c_1\dot{z}(t) + c_3\dot{z}(t)^3 + kz(t) = -m\ddot{y}(t) \quad (1)$$

Assuming harmonic input excitation and zero phase shift of the response, the harmonic base-excitation is given by

$$y(t) = Y \sin(\omega t) \quad (2)$$

This implies;

$$m\ddot{z}(t) + c_1\dot{z}(t) + c_3\dot{z}(t)^3 + kz(t) = m\omega^2 Y \sin(\omega t) \quad (3)$$

The average amount of energy (power) that is extracted by a damping device is given as

$$P_{av} = \frac{1}{T} \int_0^T F \cdot \dot{z} dt \quad (4)$$

where  $P_{av}$  is the average power extracted,  $F$  is the damper force,  $\dot{z}$  is the average velocity of the damper and  $T$  is the simulation duration. However, the damping element of interest here is the non-linear cubic damping where  $F = c_3\dot{z}^3$ . This implies

$$P_{av} = \frac{1}{T} \int_0^T (c_3\dot{z}^3) \cdot \dot{z} dt \quad (5)$$

Assuming harmonic response with  $z(t) = Z \sin(\omega t)$ , Eq. (5) can be written as

$$P_{av} = \frac{3}{8} c_3 \omega^4 Z^4 \quad (6)$$

Recall that the relative displacement of the VEH is constrained by its physical enclosure hence the maximum average power,  $P_{max}$  that can be extracted is a function of the maximum relative displacement,  $Z_{max}$  and the nonlinear cubic damping parameter  $c_3$ .

The next section briefly discusses the OFRF concept and afterwards an explicit polynomial is derived showing an analytical relationship between the output frequency response of the average power of the VEH and the parameter of interest to be designed,  $c_3$ .

### 3. System analysis, design and optimisation

In this section, the OFRF of the relative displacement of the proof mass is initially derived from the system model of Eq. (1) which is subsequently used to derive the OFRF of the harvested power. A more efficient numerical method of determining the OFRF is briefly reviewed here however an extensive analytical discussion of the OFRF concept has been done in [6, 7].

Given the Volterra system described by the differential equation in Eq. (7)

$$\sum_{m=1}^M \sum_{p=0}^m \sum_{k_1, \dots, k_{p+q}=0}^K c_{pq}(k_1, \dots, k_{p+q}) \prod_{i=1}^p \frac{d^{k_i} z(t)}{dt^{k_i}} \prod_{i=p+1}^{p+q} \frac{d^{k_i} u(t)}{dt^{k_i}} = 0 \quad (7)$$

$M$  is the maximum degree of nonlinearity and  $K$  is the maximum order of the derivative in terms of  $z(t)$  and  $u(t)$ . Also, the model parameters  $c_{0,1}(\cdot)$  and  $c_{1,0}(\cdot)$  are denoted as linear parameters, equivalent to the model linear parameters. The OFRF representation of Eq. (7) is derived in the form

$$Z(j\omega; c) = \varphi_0 + \varphi_1 \cdot c + \varphi_2 \cdot c^2 + \varphi_3 \cdot c^3 + \dots + \varphi_{N-1} \cdot c^{N-1} + \varphi_N \cdot c^N \quad (8)$$

which can be written as

$$Z(j\omega; c) = \Psi \cdot \Phi(j\omega)^T \quad (9)$$

where  $\Phi(j\omega) = [\varphi_0(j\omega), \varphi_1(j\omega), \varphi_2(j\omega), \dots, \varphi_N(j\omega)]$  is a set of complex-valued functions and  $\Psi = [1, c, c^2, c^3, \dots, c^{N-1}, c^N]$  is a set of design parameters otherwise known as the structure or monomials of the OFRF. The set of monomials can be obtained using the algorithm as employed in [6-8]

$$\Psi = \bigcup_{n=1}^N M_n \quad (10)$$

where

$$M_n = \left[ \bigcup_{k_1, \dots, k_n=0}^K [c_{0n}(k_1, \dots, k_n)] \right] \bigcup \left[ \bigcup_{q=1}^{n-1} \bigcup_{p=1}^{n-q} \bigcup_{k_1, \dots, k_n=0}^K ([c_{pq}(k_1, \dots, k_{p+q})] \otimes M_{n-q,p}) \right] \bigcup \left[ \bigcup_{p=2}^n \bigcup_{k_1, \dots, k_n=0}^K ([c_{p0}(k_1, \dots, k_{p+q})] \otimes M_{n,p}) \right] \quad (11)$$

and

$$M_{n,p} = \bigcup_{i=1}^{n-p+1} (M_i \otimes M_{n-i,p-1}), M_{n1} = M_n \text{ and } M_1 = [1] \quad (12)$$

### 3.1 Numerical determination of the OFRF for the harvested power

The system model in Eq. (3) is analysed and the following analysis has been done using the system parameters,  $m = 1\text{kg}$ ,  $k = 4\pi^2$ ,  $c_1 = 0.01\text{Ns}^3/\text{m}^3$ ,  $Y = 0.4\text{cm}$ . It is observed that the model of Eq. (3) belongs to the class of systems of Eq. (7) with  $K = 2$  and  $M = 3$ . Therefore the system parameters can be obtained as  $c_{10}(2) = m$ ,  $c_{10}(1) = c_1$ ,  $c_{30}(3) = c_3$ ,  $c_{10}(0) = k$ ,  $c_{01}(0) = -1$  other parameters being zero. The set of monomials with respect to the system output response  $Z(j\omega)$  is computed using Eq. (10), Eq. (11) and Eq. (12) as

$$\Psi = \bigcup_{n=1}^{23} M_n = [1, c_3, c_3^2, c_3^3, \dots, c_3^9, c_3^{10}, c_3^{11}] \quad (13)$$

The set of complex-valued function  $\Phi(j\omega)$  is obtained as detailed in [6, 7] using twenty one (21) sequence of values for the nonlinear damping coefficient  $c_3 = [0:0.0005:0.01]$ . This range of values is chosen as the OFRF model training parameters.

$$\Phi(j\omega) = (\psi^T \psi)^{-1} \psi^T \cdot \begin{bmatrix} Z(j\omega; c_3)|_{c_3(1)} \\ Z(j\omega; c_3)|_{c_3(2)} \\ \vdots \\ Z(j\omega; c_3)|_{c_3(21)} \end{bmatrix}, \text{ where } \psi = \begin{bmatrix} 1 & c_3(1) & \dots & c_3^{11}(1) \\ 1 & c_3(2) & \dots & c_3^{11}(2) \\ \vdots & \vdots & \ddots & \vdots \\ 1 & c_3(21) & \dots & c_3^{11}(21) \end{bmatrix} \quad (14)$$

$$\text{and } \Phi(j\omega) = [\varphi_0(j\omega), \varphi_1(j\omega), \dots, \varphi_6(j\omega), \varphi_{12}(j\omega)]$$

Therefore the OFRF polynomial of the relative displacement is computed as

$$Z(j\omega; c_3) = [1, c_3, c_3^2, \dots, c_3^9, c_3^{10}, c_3^{11}] \cdot [\varphi_0(j\omega), \varphi_1(j\omega), \dots, \varphi_6(j\omega), \varphi_{10}(j\omega), \varphi_{11}(j\omega)]^T \quad (15)$$

or

$$Z(j\omega; c_3) = \varphi_0(j\omega) + c_3 \cdot \varphi_1(j\omega) + c_3^2 \cdot \varphi_2(j\omega) + \dots + c_3^9 \cdot \varphi_9(j\omega) + c_3^{10} \cdot \varphi_{10}(j\omega) + c_3^{11} \cdot \varphi_{11}(j\omega) \quad (16)$$

$|Z(j\omega; c_3)|^2$  can be obtained using the algorithm in [8]. This is computed as

$$|Z(j\omega; c_3)|^2 = Z(j\omega; c_3) \cdot Z(-j\omega; c_3) \quad (17)$$

$$|Z(j\omega; c_3)|^2 = \varphi_0 \varphi_0^* + \sum_{l=1}^{\infty} \left( c^l \sum_{i=0}^l \varphi_i \varphi_{l-i}^* \right); \text{ where } l=11 \quad (18)$$

$$|Z(j\omega; c_3)|^2 = \sum_{i=0}^{22} c_3^i P_i$$

where  $P_i$  is the resulting coefficient of the OFRF polynomial of  $|Z(j\omega; c_3)|^2$

This algorithm is also employed in obtaining  $|Z(j\omega; c_3)|^4$  which is computed as

$$|Z(j\omega; c_3)|^4 = \sum_{i=0}^{44} c_3^i Q_i \quad (19)$$

where  $Q_i$  are the resulting coefficients of the OFRF polynomial of  $|Z(j\omega; c_3)|^4$ .

In Eq. (6), the extracted power was obtained as  $P_{av} = \frac{3}{8} c_3 \omega^4 Z^4$  which can be written as

$$P_{av} = \frac{3}{8} c_3 \omega^4 |Z(j\omega; c_3)|^4 \quad (20)$$

Substituting Eq. (19) in Eq. (20),

$$P_{av} = \lambda \cdot \sum_{i=0}^{44} c_3^{i+1} Q_i \quad (21)$$

where  $\lambda = \frac{3}{8} \omega^4$

Equation (21) shows a univariate polynomial system (OFRF of the harvested power) as a function of the nonlinear damping parameter,  $c_3$ . Using the computed OFRF polynomial, an optimal value of  $c_3$  can be designed for any desired VEH power. This can be done by finding the minimum real roots of the polynomial given any desired harvester power. Furthermore, the damping parameter required to harvest the maximum power is obtained by finding the zeros of the derivative of Eq. (21). This is computed as

$$\frac{dP_{av}}{dc_3} = \lambda \cdot \sum_{i=0}^R (i+1) \cdot (c_3^i Q_i) = 0 \quad (22)$$

The minimum, non-negative real root [9] of the polynomial in Eq. (22) was computed as  $c_{3_{nop}} = 0.0025$  for the non-optimised (nop) system and substituting this value in Eq. (19) and Eq. (21) gives  $|Z(j\omega; c_3)| = 2.863 \times 10^{-2} (m)$  and  $P_{av} = 81.56 mW$  respectively. This solution is valid for an unconstrained VEH system however most practical VEH systems are constrained in  $|Z(j\omega; c_3)|$ . This poses a nonlinear optimisation problem for a constrained nonlinear univariate polynomial system.

### 3.2 Optimisation of a constrained nonlinear univariate polynomial

The optimization of a polynomial function is usually subject to a polynomial equality and/or inequality constraints [10] and the optimization problem can be written as

$$\begin{aligned}
 & \max P_{av}(c_3) \\
 & \text{s.t. } |Z(j\omega; c_3)| - \beta \leq 0 \\
 & c_3 \in \mathbb{R}
 \end{aligned} \tag{23}$$

where  $P_{av}(c_3)$  is the objective function univariate in  $c_3$ .  $|Z(j\omega; c_3)| - \beta \leq 0$  is the inequality constraint and  $c_3$  is the design variable.  $\beta = Z_{max}$ , maximum relative displacement attainable by the VEH.

For this study,  $\beta = 2.5 \times 10^{-2} (m)$  is chosen and Eq. (23) was evaluated using the MATLAB *fmincon* function with a set of lower and upper bounds,  $a$  and  $b$  respectively defined on the design variable,  $c_3$ . Therefore the solution is always in the range  $a \leq c_3 \leq b$  where  $a = 0$  and  $b = 0.01$ . The optimal solution was obtained as  $P_{av} = 78.94 mW$  when  $c_{3_{opt}} = 0.00453 Ns^3 / m^3$  and the corresponding relative displacement obtained is  $|Z(j\omega, c_3)| = 2.446 \times 10^{-2} (m)$ .

In the next section, simulation studies are carried out and the effects of the nonlinear damping coefficient on the relative displacement and the average power harvested by the VEH are shown for both analytical (OFRF) and numerical cases.

## 4. Simulation studies

In this section, simulation results are shown and discussed for the unconstrained (not optimized) and constrained (optimized) cases. Figure 2 shows the amount of power harvested as a function of  $c_3$ . The average power harvested under unconstrained and constrained conditions are clearly identified.

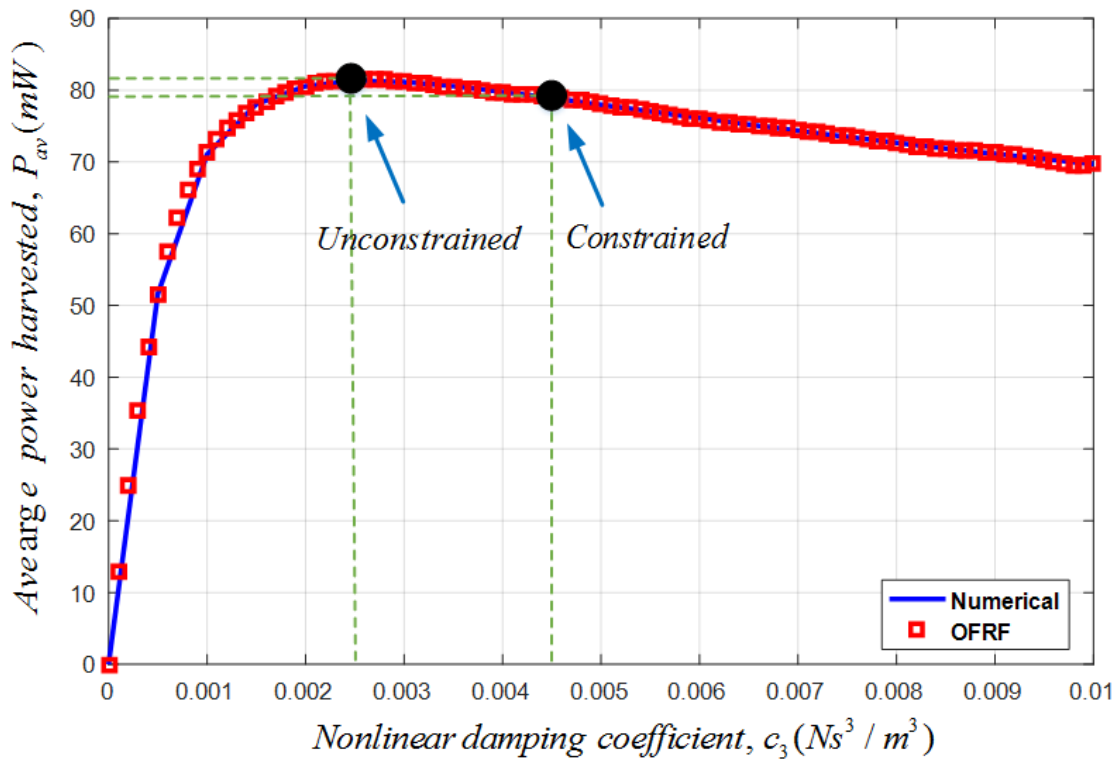


Figure 2: Effect of nonlinear cubic damping on the average power harvested by the VEH.

Figure 3 shows the effect of the nonlinear damping on the VEH relative displacement. Also, it is seen that the VEH displacement achieved using  $c_3$  obtained from the OFRF polynomial at maximum power subject to unconstrained conditions far exceeds  $Z_{max} = 2.5 \times 10^{-2} (m)$  of the VEH system. However when the constraint is considered, the optimized damping parameter obtained,  $c_{3_{opt}}$  achieves a  $Z$  value that meets the constraint.

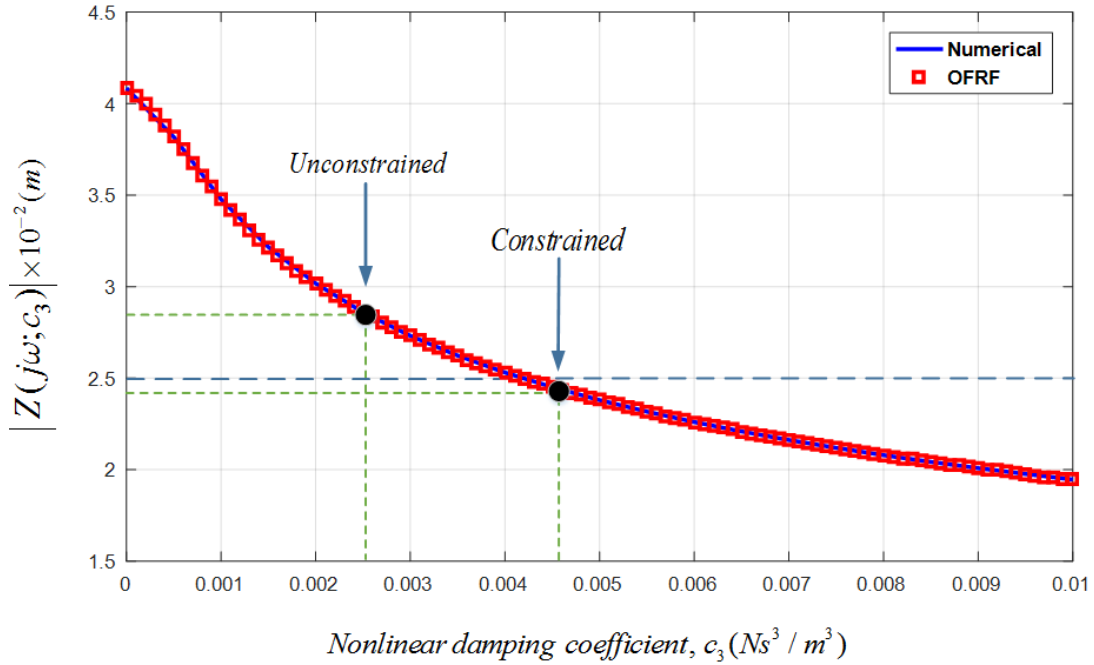


Figure 3: Effect of nonlinear cubic damping on the VEH relative displacement

It should be noted that using Eq. (18), for  $|Z(j\omega; c_3)| = 2.5 \times 10^{-2} (m)$ , the corresponding damping parameter computed is  $c_3 = 0.004184 (Ns^3 / m^3)$  which differs from the optimised value. Therefore, it is expected that due to the high order of the OFRF polynomial, some numerical errors are likely to occur particularly if the VEH system output is not well represented by the OFRF polynomial.

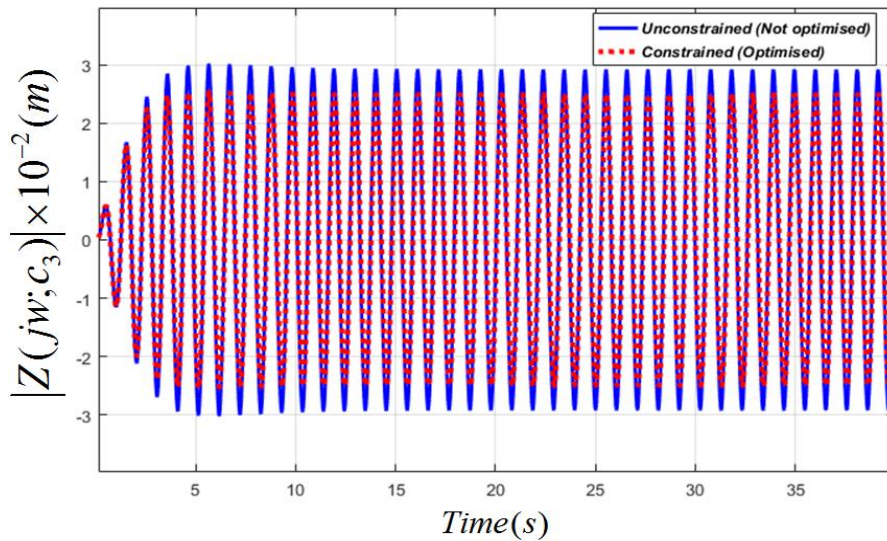


Figure 4: Relative displacement of the VEH system obtained under unconstrained (not optimized) and constrained (optimized) conditions



Figure 4 shows the time domain graph of the relative displacement obtained by the VEH system subject to unconstrained (not optimized) and constrained (optimized) conditions. The optimized graph is seen to meet the system constraints.

## 5. Conclusion

The application of nonlinear cubic damping has been revealed in the literature to extend the energy (power) harvested by a vibration-based energy harvester. However, this study focused on the application of a nonlinear frequency analysis method, the OFRF, in the analysis, design and optimization of a VEH system. It was shown that a VEH system can be modelled and analysed using the OFRF technique and with the polynomials obtained, a nonlinear cubic damping parameter can be designed for any desired energy (power) level. This is so as when a desired power level is specified, the OFRF is transformed to a univariate decreasing order polynomial. The required damping parameter is obtained by computing the minimum non-negative real roots of the polynomial. This is also applicable for predicting the corresponding VEH relative displacement achieved by the designed damping parameter. However, since most practical VEH systems are designed to attain a maximum relative displacement, a design constraint is introduced.

It was revealed that with the OFRF polynomials derived for the harvester power and VEH relative displacement, an optimization problem is easily posed and for this problem, an optimal solution was obtained for the VEH system. This solution is slightly short of the expected solution as it is expected that for high order polynomials, some numerical errors are bound to occur especially if the system model of interest is not well represented by its OFRF polynomial.

## REFERENCES

- 1 Williams, C.B. and Yates, R.B. Analysis of a micro-electric generator for microsystems, *Sensors and Actuators A: Physical*, **52** (1-3), 8-11, (1996).
- 2 Harne, R. L. and Wang, K.W. A review of the recent research on vibration energy harvesting via bistable systems, *Smart Materials and Structures*, **22** (2), 023001, (2013).
- 3 Hendijanizadeh, M., Sharkh, S. M., Elliott, S. J., Moshrefi-Torbati, M. Output power and efficiency of electromagnetic energy harvesting systems with constrained range of motion, *Smart Materials and Structures*, **22** (12), 5009, (2013).
- 4 Hendijanizadeh, M., Sharkh, S. M., Moshrefi-Torbati, Constrained Design Optimization of Vibration Energy Harvesting Devices, *Journal of Vibration and Acoustic*, **136** (2), 021001, (2013).
- 5 Tehrani, M.G. and Elliott, S.J. Extending the dynamic range of an energy harvester using nonlinear damping, *Journal of Sound and Vibration*, **333** (3), 623-629, (2014).
- 6 Lang, Z.Q. and Billings, S.A. Output frequency characteristics of nonlinear systems, *International Journal of Control*, **64** (6), 1049-1067, (1996).
- 7 Lang, Z.Q., Billings, S.A., Yue, R. and Li, J. Output frequency response function of nonlinear Volterra systems, *Automatica*, **43** (5), 805-816, (2007).
- 8 Jing, X.J., Lang, Z.Q. and Billings, S.A. Output frequency response function-based analysis for nonlinear Volterra systems, *Mechanical systems and signal processing*, **22** (1), 102-120, (2008).
- 9 Laalej, H., Lang, Z.Q., Daley S., Zazas, I., Billings, S.A. and Tomlinson, G.R. Application of nonlinear damping to vibration isolation: an experimental study, *Nonlinear Dynamics*, **69** (1), 409-421, (2012).
- 10 Rao, S.S. and Singiresu, S. R., *Engineering optimization: theory and practice*, John Wiley & Sons, (2009).